

LEE WAVE INTERFERENCE PATTERNS - Their Explanation and Exploitation for Soaring Flight

by Julian West, München, Germany

Presented at the XXIII OSTIV Congress, Borlänge, Sweden (1993)
(Abridged)

Summary

Various interference patterns appearing on satellite photographs of wave clouds over the British Isles have been investigated by computer simulation. Almost all the complex patterns seen on satellite pictures can be reproduced by using a computer to combine two or more constant amplitude cosine waves propagating along the x-axis, each with different phase shifts that vary linearly along the y-axis. Some patterns imply the presence of two phase related waves having a 2:1 wavelength ratio. Mechanisms that might account for the presence of two wavelengths with a 2:1 ratio are discussed. Optimal flight paths through such wave patterns are suggested.

1.1 Introduction

My first experience of interference effects in lee waves was in a south easterly wind on 22/10/79 at Portmoak in Scotland. The early morning sky was completely overcast until a wave gap was revealed upwind by shafts of sunlight. From above the cloud tops the gap looked like a long narrow cut, generally straight but with occasional kinks. Further gaps parallel to the first appeared and then quite unexpectedly another set of gaps appeared, but these were aligned almost perpen-

dicular to the others. As the day progressed the amount of cloud gradually reduced until the remaining wave clouds looked like chevrons. There seemed to be continuous lines of lift along the limbs of the chevrons in two directions at right angles, and it was relatively easy to track across the sky, only occasionally crossing an area of weak sink. Finally the sky became cloudless, but the lift alignments remained unchanged.

1.2 The satellite photographs

All the satellite photographs of extensive wave over the British Isles listed below were received by the NERC Satellite Station at Dundee University:-

Plate 1, NOAA 6, 22/10/79, overhead 0907 GMT, SE Wind. This shows extensive areas of rectangular herringbone formations, and some open cloud cells. This photograph is also discussed in West (1983).

Plate 2, NOAA 6, 18/04/80, overhead 0924 GMT, WNW wind. This shows overlapping diverging wake waves downwind of the Faroes with shorter wavelengths. Over Scotland, as well wave bars aligned across the wind, there are wave clouds aligned along the wind and some fine cellular formations. The UK absolute altitude record of 11,031 metres was set over Scotland on this day.

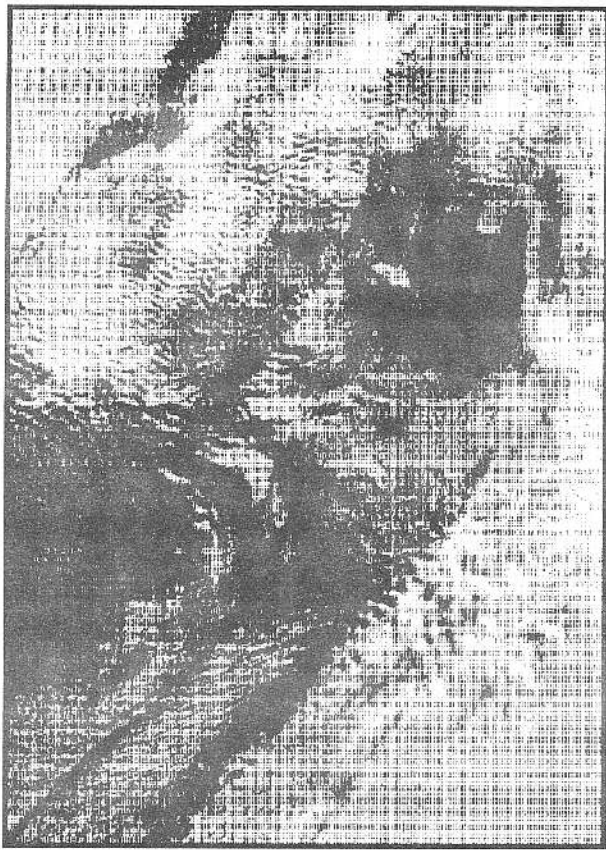


Plate 1



Plate 3

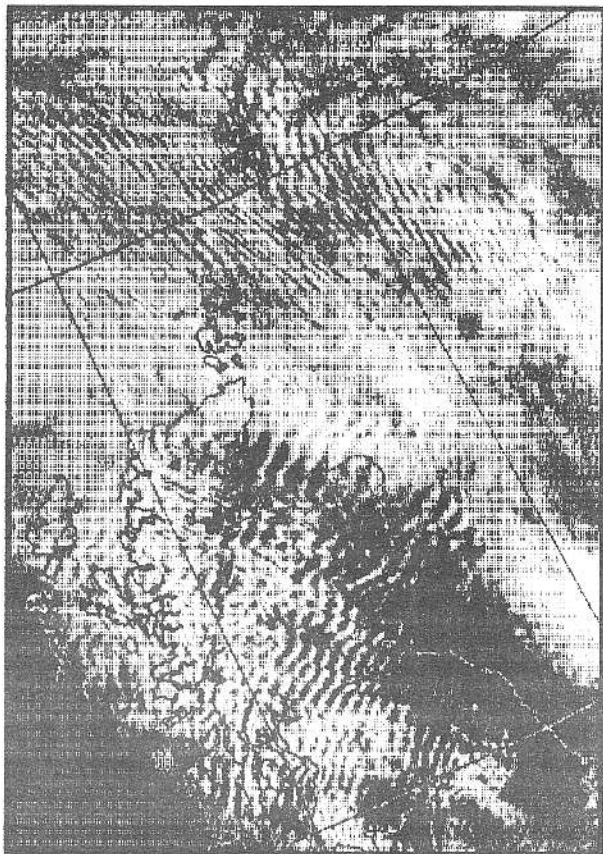


Plate 2

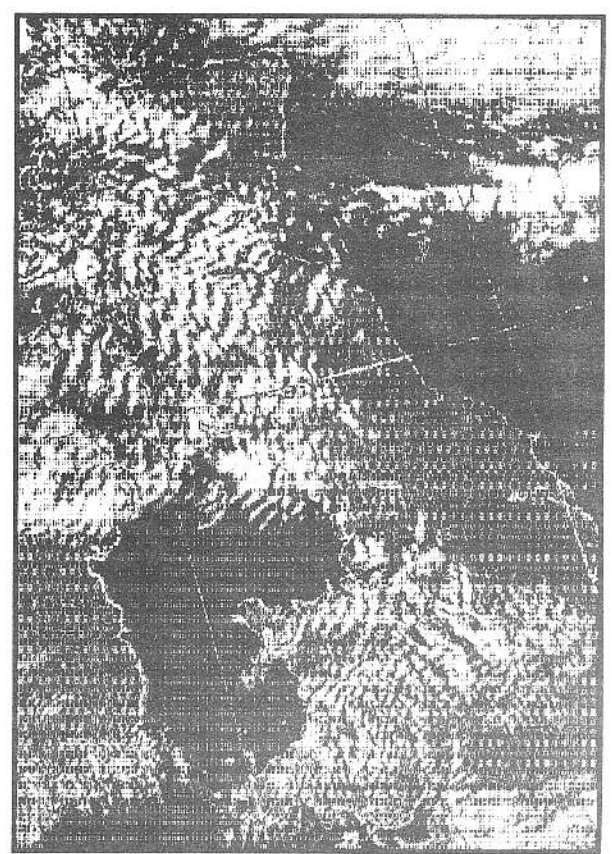


Plate 4



Plate 5

Plate 3, NOAA 6, 20/08/80, overhead 0858 GMT, W wind. This shows areas of a coarse chequered pattern, diamond-shaped cells, fine tuning fork and fine hexagonal formations. Although Brown (1983) published this photograph, no flight measurements were made that day.

Plate 4, NOAA 6, 21/08/80, overhead 0836 GMT, NW wind. This shows areas of almost rectangular herringbone formations with diamond-shaped cells, shorter wavelengths and fine cellular formations over Scotland.

Plate 5, NOAA 6, 16/06/81, overhead 0850 GMT, WNW wind. This shows extensive kinked lines of wave clouds, which run from southern Ireland to northern Scotland, and also shows some small diamond-shaped cells over Ireland.

1.3 Cloud forms

The clouds in these photographs are not lenticulars, which are smooth clouds with a lens shaped outline, but are smooth or cumuliform topped wave clouds with bases between 1 and 2 km AMSL. They are referred to by many meteorologists and most laymen as "rotor" clouds. However, this type of wave cloud is located above the rotor level, and has derived its name from the illusion of rotation caused by shear between its base and top, as is made clear in Scorer (1949).

Smooth wave clouds are normally higher colder clouds, whereas cumuliform wave clouds are lower warmer clouds. This leads to a seasonal variation of the

vertical distribution of cumuliform and lenticular wave clouds, whereby in the troposphere the former predominate in summer and the latter in winter, West (1991).

1.4 Topography

Lee wave patterns are always much less complicated than the topography that produces them. Once a wave pattern is set up by a particular topographical feature it tends to perpetuate itself downwind.

The relatively small hills and mountains of the British Isles are not a good match to longer wavelengths. The maximum lee wave amplitude occurs when the half width b of a ridge, defined as half the width at half its height, equals $\lambda/2\pi$. If the airflow is not perpendicular to the ridge then its effective width is increased. Lee waves can occur with airflows that are aligned 45° or more off the perpendicular to a ridge, especially if this enables the terrain to match the natural lee wavelength.

1.5 Lee waveform

A typical waveform for lee waves that perpetuate downwind, as measured by Larsson (1958), is illustrated in Figure 1. It shows the primary wave leaning forward until it is over the crest of the ridge, and substantially sinusoidal secondary and tertiary waves with vertical phase lines. The primary leans forwards because the mountain exerts a drag on the stream, but where the ground is horizontal it exerts no drag on the fluid and the phase lines are therefore vertical in all subsequent waves. In my work no allowance has been made for the forward displacement of primaries with height.

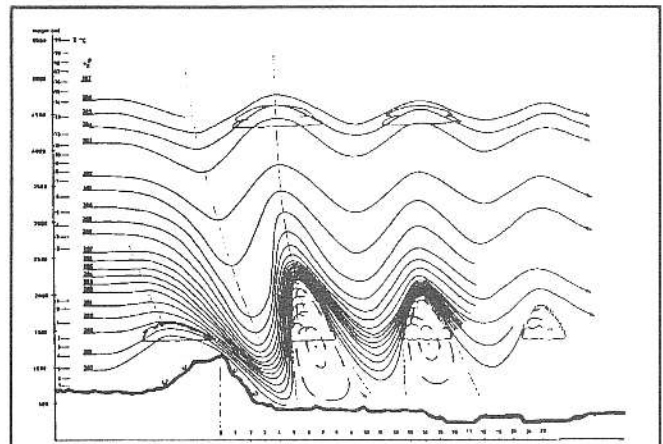


FIGURE 1. Lee wave streamlines as measured by Larsson (1958).

1.6 Computer simulation

The wave clouds are simulated by computer generated Moire patterns of wave interference, some of which are modified by rotation and/or foreshortening to give a pseudo 3D effect without perspective. The sinusoidal lines on the diagrams represent stream lines, which are lines of equal potential temperature. The wind is as-

sumed to be coming from the right, though it could just as well come from the left, and the notional ridges that generate the waves are therefore out of the picture to the right.

The lee waves patterns have been generated by combining two or more constant amplitude cosine waves propagating along the x-axis, each with different phase shifts that vary linearly along the y-axis. The patterns generated are therefore independent of any particular wave theory and do not involve any particular ridge cross-section or Scorer parameter. The wake wave patterns are similar to those of water waves, but use an amplitude function that is based on the inverse square root of the second differential of the generating function, Scorer (1978) (Ch. 5, Sec. 5.15).

2.0 Interference Patterns

2.1 Overlapping ridges

In Figure 2 the two ridges causing the interference pattern are mutually aligned at 90°. For ridges of equal height there is a checkerboard pattern of alternating squares of air displaced above or below its equilibrium level, with the raised air being shaded to represent clouds. If the wind blows symmetrically across the ridges, then the sides of the squares are $\lambda/2$ long. This type of pattern can be seen on the satellite photograph of Plate 3. If the ridges are not of equal height, then the squares link to others with kinks between.

In Figures 3 and 4 the two ridges causing the interference pattern are mutually aligned at 45°. For ridges of equal height there is a similar pattern of alternating rectangles, as shown in Figure 3. There are now paths, not shown, aligned at 45° parallel to the ridges that pass only through updraughts. Some photographs show convective cloud streets along the rift lines where the two waves cancel each other out. As before, if the ridges are not of equal height, then the rectangles link to others with kinks between, as shown in Figure 4.

With meandering wave clouds the best climb rates are to be found either at the centres of the longer sec-

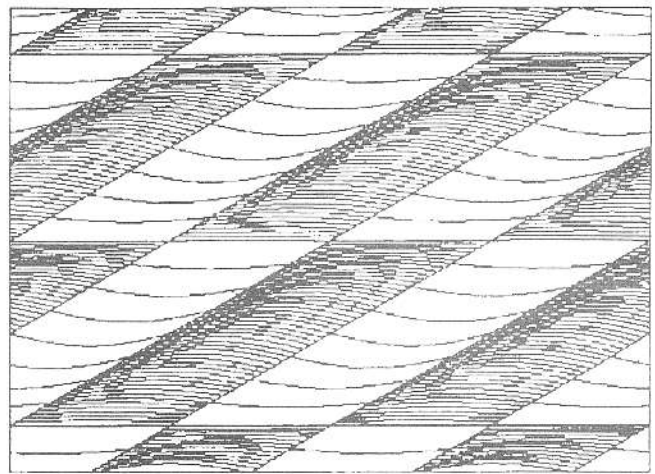


FIGURE 3. Rectangular pattern behind two equal ridges aligned at 45°.

tions, or at the bulges on them. This particular type of interference pattern is very common and is particularly prominent on the satellite photograph of Plate 5. It is this effect which enables waves from ridges that are geographically separated, but overlap along the wind direction, to link together across the wind forming wave bars that are several hundred kilometres long.

Lenticulars can be generated by interference between waves from overlapping ridges. If the air is too dry for continuous wave bars, then individual lens shaped clouds will form instead, as shown by the shading in Figure 5.

It can be shown mathematically that the optimum flight paths through ladder systems are not parallel to the sides of the updraught squares or rectangles, but along their diagonals parallel to the ridges generating the wave. These paths cross the centres of the cloud ends, as in Figure 2. With meandering wave clouds it is best to fly straight along the general direction of a wave cloud rather than to follow its meanders.

This type of wave pattern is also exemplified by a

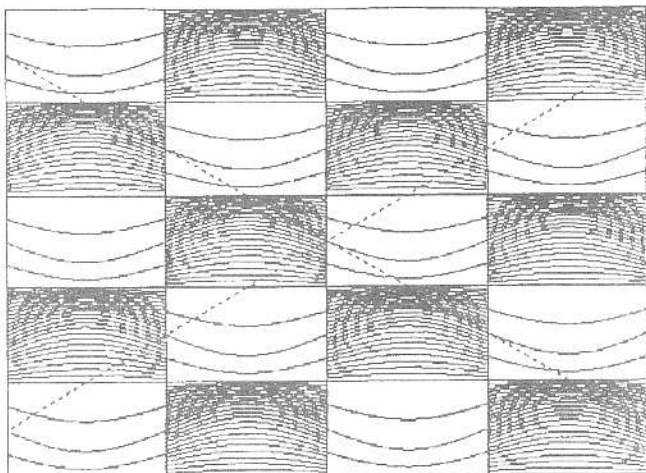


FIGURE 2. Checkerboard pattern behind two equal ridges aligned at 90°.

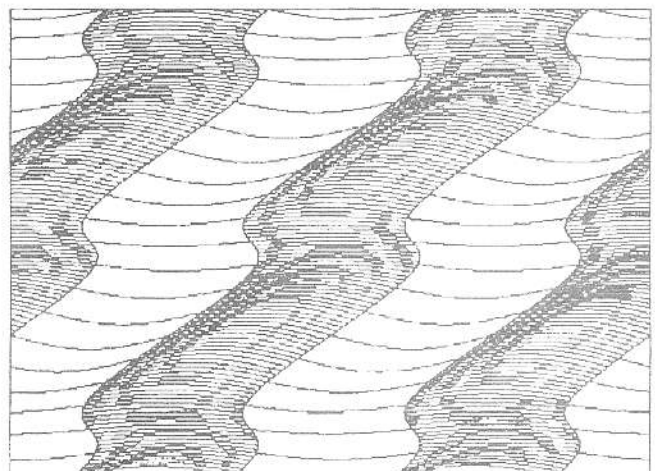


FIGURE 4. Meandering wave bars behind two unequal ridges aligned at 45°.

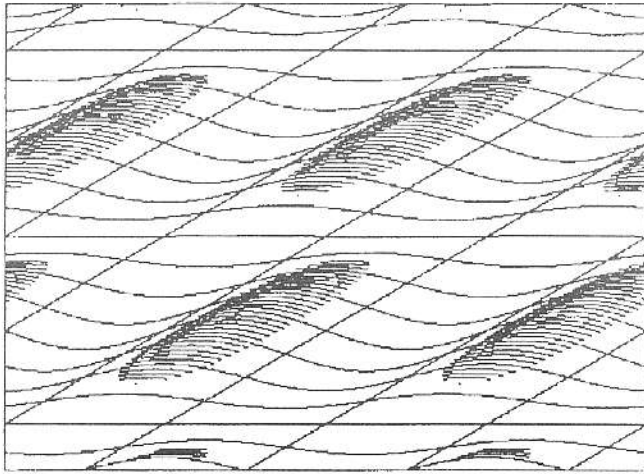


FIGURE 5. Lenticulars behind two equal ridges aligned at 45°.

flight over the Steiger forest in Germany on 16/5/86. A weak thermal was located above a prominent radio mast near the centre of the forest. Although there appeared to be no wind at all low down, after reaching cloudbase it was possible to climb in clear air to the west of a shallow cumulus cloud, part of a street aligned north-south. There were other similarly aligned streets further to the west. The pattern of clouds as a whole appeared to have a series of cuts across it aligned east-west. There seemed to be a cloudless second wave alignment, which was at right angles to the cumuliform wave bars extending north-south. It was possible to proceed against the light northwesterly wind by following a zigzag path above the clouds using these two alignments almost all the way to Gmunden some 70 km upwind of the radio mast. A couple of hours later the sky was invaded by a thick cirrus sheet that preceded a weak warm front approaching from the southwest.

2.2 Overlapping valleys and ridges

A broad valley can act as an inverted (negative) ridge, and Figures 6 to 8 show a valley "a" at 45° to a ridge "b".

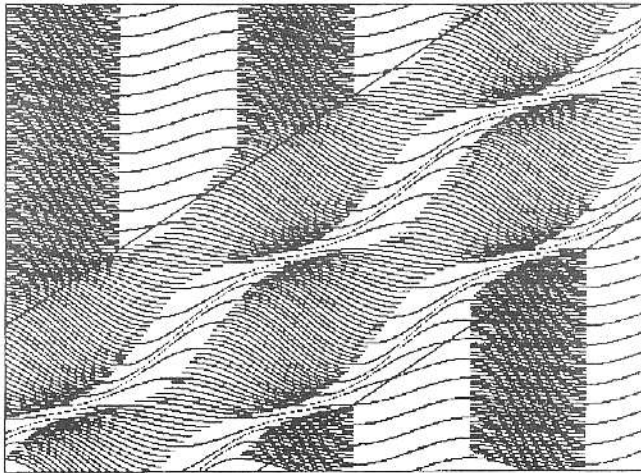


FIGURE 6. Lift pattern (shaded) along a valley ("a" > "b") aligned at 45°.

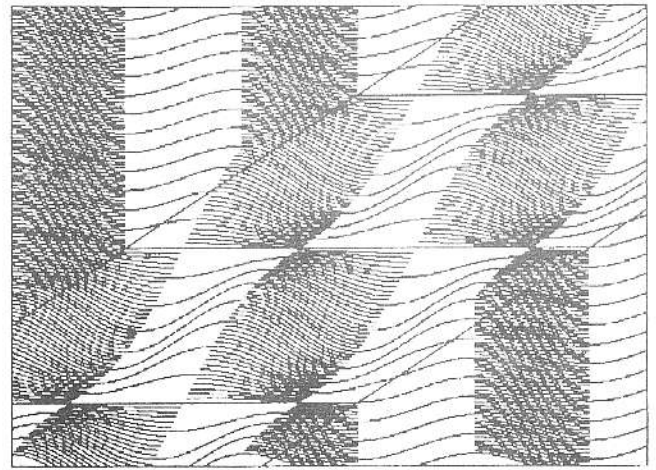


FIGURE 7. Lift pattern (shaded) along a valley ("a" = "b") aligned at 45°.

In these figures the shading does not represent clouds but rising air. These diagrams indicate the effect of the E-W aligned Aosta valley in Italy on the wave from the NE-SW Mont Blanc ridge alignment upwind. There are three possibilities, "a" > "b", "a" = "b", and "a" < "b". It has been assumed that the valley is 2.1 wide, and that rotors occur in all cases. If "a" > "b", as in Figure 6, then there is a single rotor with kinks that meanders down the middle of the valley and the two dotted lines show the optimum paths through a continuous updraught parallel to the valley sides. However, if "a" = "b", as in Figure 7, there are several rotors at an angle across the valley, and two optimum paths, shown by the dotted lines, parallel to the valley sides which include no downdraught, although the updraughts fall to zero periodically. If "a" < "b", as in Figure 8, there are rotors at a greater angle across the valley, and again two optimum paths, shown by the dotted lines, parallel to the valley sides with downdraught sections that are shorter and weaker than those of updraught. In each figure the optimum paths are in exactly the same posi-

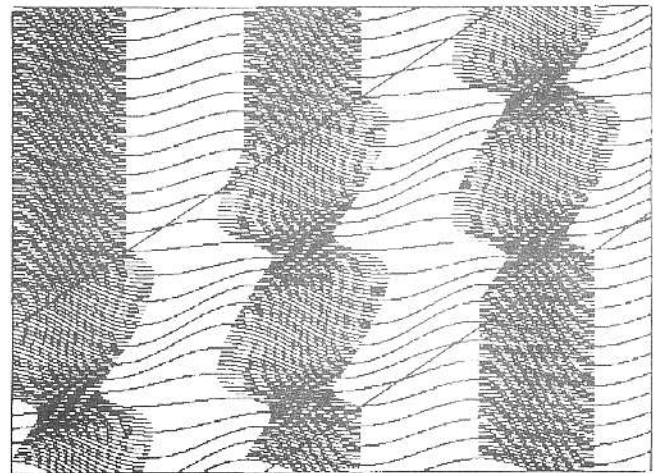


FIGURE 8. Lift pattern (shaded) along a valley ("a" < "b") aligned at 45°.

tions.

This effect is exemplified by a wave flight at Aosta in Italy on 18/2/88, which probably corresponds with Figure 7. To the west of Aosta there were a series of rotors, which extended northeast-southwest diagonally across the valley and gave a 5 m/s climb over 2,000 metres. At about 3,000 metres AGL, the height of the adjacent mountain ridges, smooth wave lift to 4,000 metres was encountered. There was also a continuous line of lift along the downwind side of the Aosta valley. Following this gave periodic variations of the climb rate, and more height was gained while proceeding westwards towards Mont Blanc. The lack of sink was probably due to the proximity of the downwind side of the valley. At a lift maximum a side valley before Mont Blanc was entered, where a climb in the secondary wave to 6,900 metres AGL was made directly downwind of Mt Blanc. Apart from a thin sheet of cirrus above, which had drifted across during the flight, the sky was cloudless.

2.3 Lee wave with 2nd harmonic component

Although many patterns can be created by overlapping ridges, the "X-clouds", "Y-clouds", "diamond" and "hexagonal" cellular formations that appear in satellite pictures, such as Plate 1, are caused by another type of wave interference. These cloud patterns cannot be created from a combination of cosine waves having a single wavelength. There must be another wavelength present that is exactly half that of the main lee wave. Indirect evidence of this 2nd harmonic appears on many satellite photographs, and its occurrence is probably fairly common amongst lee waves generated over the British Isles.

Several of my own flight experiences indicate that unmarked lift can be encountered about two thirds the way across the gap between wave clouds, as depicted in Figure 9, which is what would be expected if a half wavelength were present.

This effect was particularly pronounced during a wave flight from Fuentemilanos in Spain on 28/7/87. It

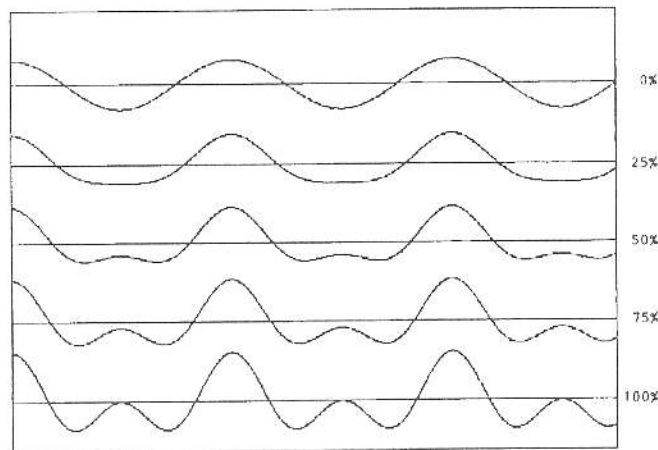


FIGURE 9. Lee waveforms when various proportions of $\text{Cos}(2\theta)$ are added.

was mid afternoon and a massive continuous cloud street ran parallel to the mountains located to the south-east about 20 km away. There was a similar massive cumulus street nearer to the mountains, and radio reports of wave lift to 3,500 metres AGL were received. After failing to reach cloud base I made a move from the secondary towards the primary. When only about two thirds the way across, weak but smooth lift was encountered in the blue between the two streets. This wave was then used to fly to Riazza, which is 77 km from Fuentemilanos.

By incorporating a second in phase wavelength in the computer model, it is possible to determine the effects of an additional lee wavelength. The effect on a cosine waveform of various amounts of 2nd harmonic are illustrated in Figure 9. If its amplitude is only 25% of that of the fundamental, then the wave has a sharp peak and a blunt trough without a double bottom. At greater amplitudes the basic waveform is a distorted sine wave with major peaks spaced as before but sharper, but now with troughs that have a double bottom. Provided the amplitude of the 2nd harmonic is less than that of the fundamental, the streamlines of the minor peaks do not extend above the equilibrium level, and clouds are unlikely to form there. Thus a minor 2nd harmonic component in a lee wave will not normally betray its presence by cloud formation. Since clouds intermediate the major peaks do not appear on satellite photographs, presumably this is usually the case.

Various integer and non integer ratios have been tried, but only a 2:1 ratio produces observed patterns. Since none of the calculated patterns have been found in satellite photographs, it is concluded that other integer and non integer frequency ratios with substantial amplitudes do not often, if ever, occur in practice.

When one ridge dominates the other, 33% of 2nd harmonic causes the rounded widenings on the cloud streets of Figure 4 to become more rectangular, and this effect can be seen on Plate 1.

2.4 Shear Waves

Some satellite photographs show direct evidence of two wavelengths at the same level. These wavelet clouds seem to be at the same level as the main wave clouds, but only appear along a rift line where the main wave is cancelled by interference. It is possible to produce similar wavelets along the rift lines of a straightforward interference pattern, such as in Figure 3, by adding a set of out of phase shear waves with a much shorter wavelength aligned transversely to the wind. When the angle bisector of the two ridge lines is perpendicular to the wind, fingers of cloud appear at the ends of the wave clouds, as in Figure 10. However, if this bisector is angled by 15° or more away from the perpendicular, then separate wavelets appear between the main wave bars.

On the satellite photographs for, 18/04/80, 20/08/80 and 21/08/80, Plates 2, 3 and 4, there are areas with fine

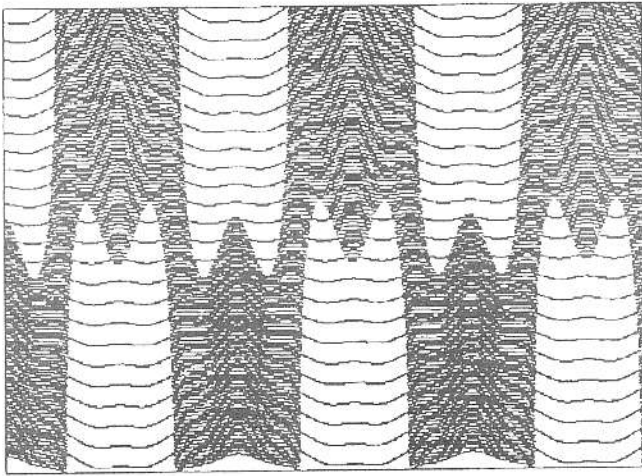


FIGURE 10. Fingers on wave bar ends at a rift line with 25% of 4:1.

patterns of hexagonal cloud cells, and some of the major wave bars also have a cellular structure. These are presumably produced in a similar way to the larger hexagonal cells in lee waves, which would imply the presence of relatively short wavelengths with a 2:1 ratio and two wavefronts that are aligned at an angle.

2.5 Centrifugal waves

Some satellite photographs reveal waves aligned almost along the wind, and these are particularly prominent in Plate 2, although they also appear in places on Plate 1. These are most probably centrifugal waves aligned along the wind shear, as illustrated in Figure 6.1.iv of Scorer (1972). These waves occur when the centrifugal forces due to the curvature of the airflow and the shear together are enough to overcome the static stability. If the centrifugal wave bars are continuous and the lee wave bars are not, then the former must have a greater amplitude than the latter. However, if there a 2:1 wavelength component present in the lee waves, it is possible for both types of wave bar to be continuous. A possible combination of these waves is illustrated in

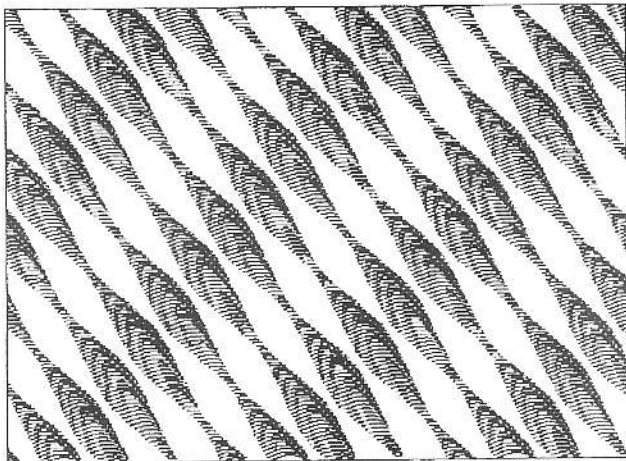


FIGURE 11. Centrifugal waves (4:1) dividing wave bars along the wind.

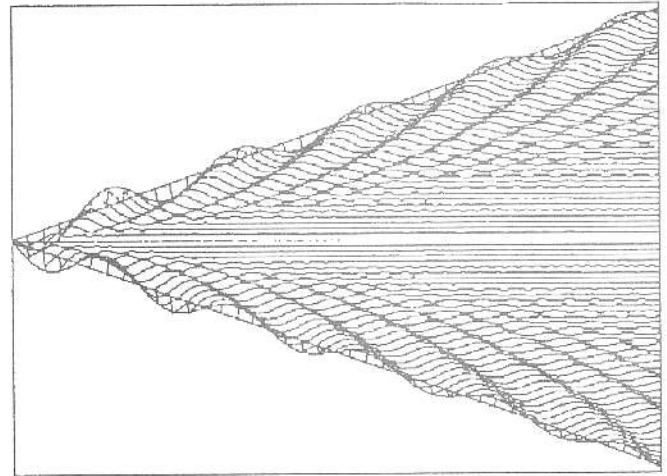


FIGURE 12. Diverging $\sin(\theta)$ wake waves behind an isolated peak.

Figure 11. Perhaps it is a combination of shear and centrifugal waves, which will tend to be mutually perpendicular and to have the same wavelengths, that leads to the hexagonal cells observed in Plates 2, 3 and 4.

2.6 Wake Waves

Wake waves, generated by isolated peaks, are created by interference between the waves generated by the various angles of the mountainsides. The pattern spreads out downwind in a wedge with an apex angle that is 39° for waves on water, but varies between 5° and 90° for waves in air. The wave pattern includes both the diverging (bow) waves of Figure 12 and the transverse (stern) waves of Figure 13. Normally only one or other of these wave types appears to be present in satellite pictures. When both are present there is a 90° phase difference between them, since one starts off at the peak as a cosine and the other as a sine wave. The pattern is rather confused where the two wave types overlap and so has not been illustrated. According to Scorer and Wilkinson (1956), an oval peak will favour diverging

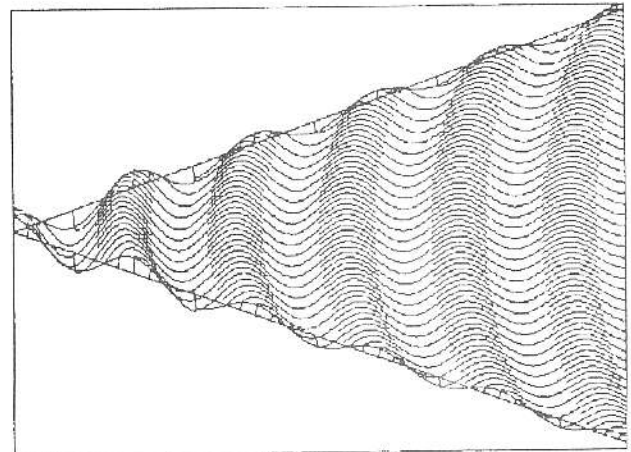


FIGURE 13. Transverse $\cos(\theta)$ wake waves behind an isolated peak.

waves when its major axis lies across the wind and transverse waves when this axis lies along the wind, and for a round peak the transverse waves are stronger than the diverging waves. However, the level of the inversion seems to play a more significant role in determining which type of wave dominates. In principle both types of waves can be created by either the bow or the stern of the mountain. However, the windward (bow) side of a mountain is a more efficient generator of diverging (bow) waves, and similarly the lee (stern) side is a more powerful generator of transverse (stern) waves.

With wake waves the wavelength is only constant along lines extending through the generating peak, and as they are an interference pattern they may reveal the presence of any second wavelength. Interestingly for shorter in phase waves the diverging sine waves will show 2:1 but not 3:1 wavelength ratios, and the transverse cosine waves will show 3:1 but not 2:1 ratios.

2.7 Herringbone formations

Chevron shaped wave clouds with sharp corners can be caused by the perpendicular intersection of either two ridges or two valleys, and this is a topographical rather than an interference effect. Although this produces a single sharp corner, it is not likely to produce a series of them as observed on some satellite photographs. If at first one ridge and then the other totally dominates, such that at first "a" >> "b" and then "b" >> "a", then it would seem unlikely for the changeover point to occur exactly where the wavefronts were exactly in phase, as shown in Figure 14. Thus the formation of the prominent herringbone patterns on Plate 1 for 22/10/79, is still not satisfactorily explained.

With sharp herringbone formations the best climb rates are to be found at the corners, where the two wavefronts are in phase. The optimum paths are quite clear, and it is only necessary to fly along either the wave clouds or imaginary extensions thereof. Herringbone patterns are particularly suitable for triangular tasks, as they enable "tacking" upwind while flying in lift.

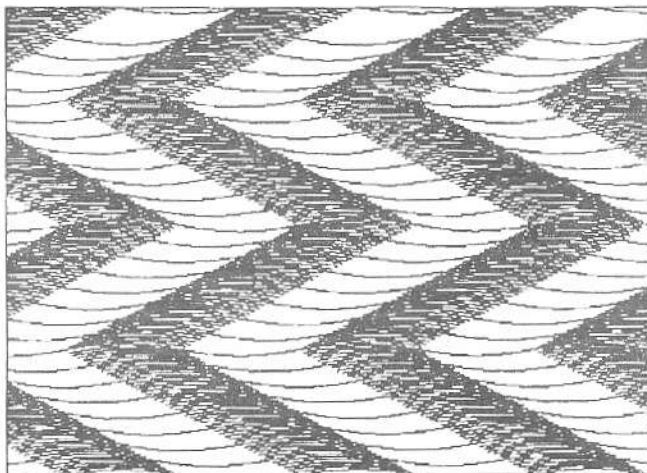


FIGURE 14. A marked herringbone pattern not caused by interference.

3.0 The theory of trapped waves

A good summary of linear wave theory, including all the relevant equations, is given by Smith (1979) and is not repeated here. Although linear theory tends to underestimate wave amplitudes it does predict wavelengths rather well. Non-linear wave theory, as used by Peltier and Clark (1983), is beyond the scope of this paper.

3.1 Waves at a stability discontinuity

In suitable conditions lee waves can occur at a discontinuity of stability. For the wave equation to have one or more real solutions, so that an infinite train of lee waves can develop, the Scorer parameter must decrease upwards. If the Scorer parameter increases with height, although there can be no real solution, there may still be a complex solution that implies a finite wave train that decays exponentially downwind.

Following equations (17) to (21) of Corby and Sawyer (1958) for 2-, 3- and 4-layer models, the general formula for an n-layer model can be derived:-

$$f(k) = f_{1n} / f_{2n}$$

where

$$f_{1n} = X_n + iY_n \\ f_{2n} = X_n - iY_n$$

and where
1Y_{n-1}

$$X_n = u_{n-1} X_{n-1} - u_{n-1} t_{n-1} Y_{n-1}$$

$$Y_n = u_n t_{n-1} X_{n-1} + u_n Y_{n-1}$$

and initially

$$f_{12} = u_1 t_1 + iu_2 = X_2 + iY_2 \\ f_{22} = u_1 - iu_2 t_1 = X_2 - iY_2$$

where $u_n = + (1/n^2 - k^2)^{1/2}$; $t_n = \tan(u_n h_n)$; $1_n^2 = g\beta_n / v^2$; $\beta_n = (1/\theta) d\theta/dz$ for the nth layer; θ is the potential temperature; and h_n is the depth of the nth layer.

The wavelengths are given by the real roots of $f_{2n} = 0$ in each case and the amplitudes are proportional to $f_{1n} / (df_{2n}/dk)$. To give an insight into their behaviour, these equations are best solved graphically, as in Figure 15. The real roots occur where the curves cross the x-axis. The curves also touch the x-axis, that is $f_{2n} = 0$, at the resonant frequencies of stable layers. However, at these points both f_{1n} and $1/(df_{2n}/dk)$ equal zero and these "solutions" have zero amplitude.

The 2-layer model, Scorer (1949), is rather unrealistic and will not be considered further.

Much better results are obtained with a 3-layer model, in which a convection layer is inserted below those of the two layer model, can give two solutions with frequency doubling and so could account for a 2:1 wavelength ratio. The equation for the three layer model is:-

$$u_2 (u_1 - u_2 \tan(u_1 h_1) \tan(u_2 h_2)) \\ - iu_3 (u_1 \tan(u_2 h_2) + u_2 \tan(u_1 h_1)) = 0$$

The imaginary number i can be eliminated from this

equation by the relations $i^2 = -1$ and $i \tan(ix) = -\tanh(x)$.

Certain important aspects of the behaviour of the real roots of the equation $f_{23} = 0$ are determined by the value of the dimensionless Froude number ($Fr = h_2/12$) of the stable layer.

For certain values of Fr there is an integer relationship between these two real solutions. For example, if $h_1 = 2$ km then $Fr = 4.55$ for 2:1, 3.98 for 3:1, 3.70 for 4:1, 3.65 for 5:1 wavelength ratios and so on. These figures vary, but only slowly, with the value of h_1 .

If $h_1 = 2$ km and $13 = 0.33$ km⁻¹, the following relationships for double wavelengths are valid: - For $l_1 = 2$, $\lambda_2/\lambda_1 = 0.6383$, $\lambda_1/12 = 7.13/\lambda_1$; and $12 = 4.55/h_2$, and assuming an isothermal layer this gives the values of h_2 and 12 for various wavelengths as shown in Table 1.

λ_1 km	λ_2 km	h_2 km	l_2 km ⁻¹
3	6	1.91	2.38
4	8	2.55	1.78
5	10	3.19	1.43
6	12	3.83	1.19

TABLE 1.

It should be noted that this table indicates that either a relatively thick stable layer or a relatively high Scorer parameter is necessary for two wavelengths having a 2:1 ratio.

When climbing at high altitude in wave it is not unusual to pass through a second inversion, the base of which is indicated by a brownish line on the horizon, and this situation can be simulated by a 5-layer model. A second stable layer that lies between 2 and 4 km higher than the first can give two wavelengths, with the first wavelength virtually unchanged from that for the 3-layer model, as shown in Figure 15.

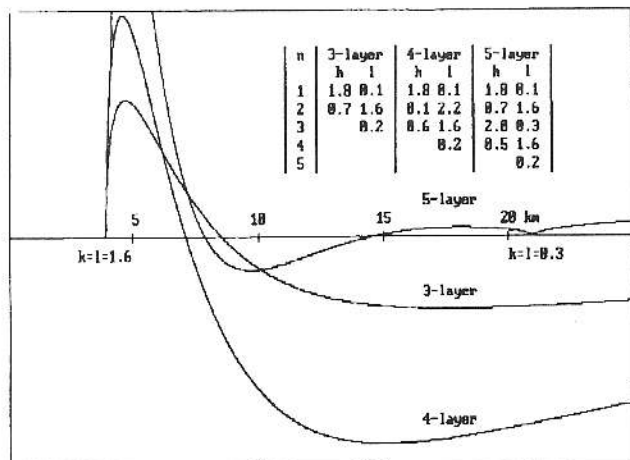


FIGURE 15. Function f_{2n} plotted against λ for various n -layer models.

The effect of the stratosphere can be found from a 5- or 7-layer model. This introduces a longer wavelength of significant amplitude and numerous smaller wavelengths of negligible amplitude. The solutions for the 3- or 5-layer models are repeated, which agrees with the findings of Corby and Sawyer (1958).

3.2 Inversion resonance

Another possible cause of a 2:1 wavelength ratio is a resonance of a stable layer. The function f_{2n} may have a real solution ($f_{2n} = 0$) when $k = 1/m$, the natural wavenumber of an inversion m . In the 3-layer model the inversion resonance at $k=12$ is such a solution. This solution has zero amplitude ($f_{13}/df_{23}/dk$), since f_{13} is zero and df_{23}/dk is infinite at this wave number.

If $h_1 = 2$ km and $13 = 0.33$ km⁻¹, the following relationships for double wavelengths are valid: - For $l_1 = 2$, $h_2 = 0.1685$, $l_1/12 = 7.13/l_1$; and $12 = 1.21/h_2$, and assuming an isothermal layer this gives the values of h_2 and 12 for various wavelengths as shown in Table 2.

λ_1 km	λ_2 km	h_2 km	l_2 km ⁻¹
3	6	0.57	2.10
4	8	0.77	1.57
5	10	0.97	1.255
6	12	1.16	1.045

TABLE 2

A marked inversion, rather than an isothermal layer, could double 12 in this table, requiring an inversion depth of only half the quoted h_2 for the same effect. It should be noted that this table indicates that a combination of a relatively thin stable layer and a relatively normal Scorer parameter is necessary for two wavelengths having a 2:1 ratio. This is more likely to occur than either a relatively thick stable layer or a relatively high Scorer parameter, as indicated in Table 1 above.

In Spain the author has soared inversion waves on several occasions and found that, unlike lee waves, they appear to be limited to the inversion layer and that, like lee waves, they seem to be stationary. An inversion can be entered from above by climbing high above a mountain, and then flying out over a plain where the inversion is lower. Strong thermals can raise the inversion locally, so that between them the inversion is below cloudbase, making it possible to enter an inversion from the side. An inversion wave can then enable the next cloud to be reached without loss of height. The suggestion that such waves are topographically induced, Carruthers and Hunt (1986), is consistent with the author's experience that these waves have the same alignment as ground features located upwind.

3.3 Waves at a density discontinuity

Trapped waves can also occur at a density (temperature) discontinuity as well as at a static stability discontinuity, as described on page 180 of Scorer (1978). Temperature discontinuities can arise from radiative heat loss from the cloud tops and from undulating motion at the top or bottom of cloud layers, Scorer (1953). This type of wave does not require the Scorer parameter to decrease with height.

The data for 22/10/79 reveals the existence of a very sharp inversion with $dT = 11^\circ \text{C}$ beneath a weak inversion, whereas the minimum value of dT necessary for waves is just 10°C . This suggests the possibility of a solution at, or very close to, the natural wavelength of the inversion, which would tend to be reinforced by a resonance of this layer.

3.4 Comparison with radiosonde data

Radiosonde data need to be treated with caution, since balloon ascents are affected by passage through waves. In an ascending current stability will appear to be reduced and in a descending current it will appear to be increased. According to Scorer (1953) this might cause spurious inversions to appear in the data. However, Corby (1957) suggests that the main effect is to change the level or intensity of strong inversions rather than to create completely spurious ones.

A study of radiosonde data for days with double frequency wave interference indicates that such days have one or two relatively thin inversions with relatively low Scorer parameters. A 3- or 4-layer model gives only a single solution, if at all, with a wavelength (circa 10 km) corresponding closely to that observed on the satellite pictures. However, the resonant wavelength of the stable layer in the 3-layer model or the thicker upper stable layer in the 4-layer model is much shorter (circa 5 km), being close to that required to produce the observed interference patterns. Often there is a very sharp inversion only 100 metres thick with a weak 0.5

km inversion layer above, as shown in Figure 16.

4.0 Conclusions

It seems that many common cloud patterns, such as ladder-like formations and meandering cloud lines, that can be seen on satellite photographs are caused by interference between two or more angularly disposed linear wave fronts. These wave fronts are generated by major non-parallel ridges and valleys that form part of the general topography.

Some less common cloud patterns, such as hexagonal cells, are caused by interference between two angularly disposed wave fronts, each comprising two wavelengths of similar amplitudes with a 2:1 wavelength ratio. Other, finer patterns are caused by the presence of shorter shear and centrifugal waves unrelated to the lee waves.

In terms of the lift sink distribution, the optimum flight paths through lee wave interference patterns run parallel to the ridges or valleys generating the waves. These paths can even cross at right angles, giving an ideal pattern for soaring around triangular tasks.

When interference due to the presence of two lee wavelengths with a 2:1 ratio occurs, the additional wavelength is most likely to be a resonance of the inversion causing the lee wave. This resonance may be reinforced by waves at a density discontinuity due to a sharp shallow inversion at the base of the main inversion. A resonance of this shallow inversion may be responsible for shear and centrifugal waves having wavelengths with a 2:1 ratio. With an integer ratio between wavelengths energy can be exchanged between the two wavemodes, tending towards equalisation of their amplitudes.

Acknowledgements

The author would like to thank Mr T.M. Bradbury, UK Met. Office ret'd., who supplied the radiosonde data, Dr. F. Berkshire of Imperial College, Prof. P. Jonas and Dr. I. Stromberg of UMIST, and Dr. T. Hauf of DFVLR Wessling for holding discussions on this topic with the author.

References

- Brown, P.R.A. (1983), "Aircraft measurements of mountain waves and their associated flux over the British Isles", *Q.J.R.Met.Soc.* 109, 849-866.
- Carruthers, D.J. and Hunt, (1986), *J. Fluid Mech.* 165, 475-501.
- Corby G.A. (1957), "A preliminary study of atmospheric waves using radiosonde data", *Q.J.R.Met.Soc.* 83, 49-60.
- Corby, G.A. and Sawyer, J.S. (1958), "The airflow over a ridge - the effects of the upper boundary and high level conditions", *Q.J.R.Met.Soc.* 84, 25-37.
- Larsson, L. (1958), "A method to study the structure of lee waves and rotors", 7th OSTIV Congress, Lezno, Poland.
- Peltier, W.R. and Clark, T.L. (1983), "Non linear mountain waves in two and three spatial dimensions", *Q.J.R.Met.Soc.* 109, 527-548.

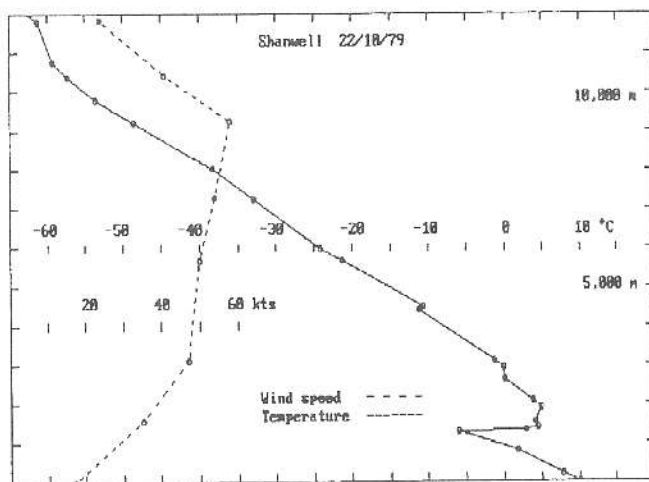


FIGURE 16. Data from the Shanwell ascent at 1200 on 22/10/79.

- Scorer, R.S. (1949), "Theory of waves in the lee of mountains", *Q.J.R.Met.Soc.* 75, 41-56.
- Scorer, R.S. (1953), "Theory of airflow over mountains The flow over a ridge", *Q.J.R.Met.Soc.* 79, 70-83.
- Scorer, R.S. and Wilkinson M. (1956), "Waves in the lee of an isolated hill", *Q.J.R.Met.Soc.* 82, 419-427.
- Scorer, R.S. (1972), "Clouds of the World", Chap. 6. Publisher: David and Charles, Newton Abbott.
- Scorer, R.S. (1978), "Environmental Aerodynamics", Chap. 5. Publisher: Ellis Horwood, Chichester.
- Smith, R.B. (1979), "The influence of mountains on the atmosphere", *Advances in Geophysics* 21, 87-230.
- Wallington, C.E. (1983), "Developments in gliding meteorology", *Gliding International* Feb. 1983, 7-10.
- West, J.M. (1983), "Herringbone wave cloud patterns", *Weather Magazine*, Jan. 1983, 28-30.
- West, J.M. (1991), "Wellen-oder Rotorwolke? Mißdeutete Zeichen am Himmel", *Aerokurier* Feb. 1991, 124-125.